

RGB-Event based Pedestrian Attribute Recognition: A Benchmark Dataset and An Asymmetric RWKV Fusion Framework

Xiao Wang¹, Haiyang Wang¹, Shiao Wang¹, Qiang Chen¹, Jiandong Jin²,
Haoyu Song¹, Bo Jiang^{1*}, Chenglong Li²

¹School of Computer Science and Technology, Anhui University, Hefei, China

²School of Artificial Intelligence, Anhui University, Hefei, China

why2434961256@163.com, {xiaowang, jiangbo}@ahu.edu.cn, wsa1943230570@126.com,
{e23301220, e22214005}@stu.ahu.edu.cn, {jddinahu, lcl1314}@foxmail.com

Abstract

Existing pedestrian attribute recognition methods are generally developed based on RGB frame cameras. However, these approaches are constrained by the limitations of RGB cameras, such as sensitivity to lighting conditions and motion blur, which hinder their performance. Furthermore, current attribute recognition primarily focuses on analyzing pedestrians' external appearance and clothing, lacking an exploration of emotional dimensions. In this paper, we revisit these issues and propose a novel multi-modal RGB-Event attribute recognition task by drawing inspiration from the advantages of event cameras in low-light, high-speed, and low-power consumption. Specifically, we introduce the first large-scale multi-modal pedestrian attribute recognition dataset, termed EventPAR, comprising 100K paired RGB-Event samples that cover 50 attributes related to both appearance and six human emotions, diverse scenes, and various seasons. By retraining and evaluating mainstream PAR models on this dataset, we establish a comprehensive benchmark and provide a solid foundation for future research in terms of data and algorithmic baselines. In addition, we propose a novel RWKV-based multi-modal pedestrian attribute recognition framework, featuring an RWKV visual encoder and an asymmetric RWKV fusion module. Extensive experiments are conducted on our proposed dataset as well as two simulated datasets (MARS-Attribute and DukeMTMC-VID-Attribute), achieving state-of-the-art results. The source code and dataset will be released on <https://github.com/Event-AHU/OpenPAR>

1. Introduction

Existing Pedestrian Attribute Recognition (PAR) [44] systems are typically developed using RGB frame cameras, with the goal of enabling a model to accurately select matching attributes from a predefined list based on a given pedestrian image or video. Common attributes include *appearance information* such as hairstyle, gender, upper and lower body clothing, and carried objects. With the advancement of artificial intelligence technology, pedestrian attribute recognition has garnered increasing attention and is now widely applied in various human-centric visual tasks, including pedestrian detection and tracking [27, 28, 43, 48], person re-identification [13, 42, 55], and text-image retrieval [10, 53, 64] for pedestrians. Despite significant progress, the overall performance of these systems remains constrained by the inherent limitations of RGB cameras, such as sensitivity to lighting conditions, clutter background, and susceptibility to motion blur. Interestingly, while multi-modal fusion has been extensively adopted in other computer vision tasks [35, 50, 52], it is surprising that pedestrian attribute recognition still predominantly relies on single-modality RGB cameras. This limitation highlights an opportunity for innovation through the integration of additional modalities to address the existing performance bottlenecks.

On the other hand, the pedestrian attributes defined in existing PAR benchmark datasets focus on describing the visible appearance cues, but none of them consider the invisible *emotion information*, which is also very important for human-centric perception. Recognizing emotions such as anxiety, anger, or joy can help the system better understand pedestrian behavioral intent and enhance the naturalness of human-computer interaction, improve safety and risk assessment, and support personalized services. Incorporating emotion analysis into pedestrian attribute recognition tasks can make the system smarter and more human-

*Corresponding Author: Bo Jiang

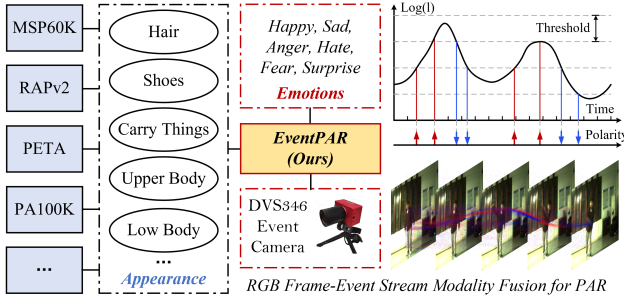


Figure 1. (left) Comparison between existing PAR datasets and our newly proposed EventPAR; (right) Imaging principle and results of Frame and Event cameras.

centric, while also providing support for a broader range of practical application scenarios.

In this work, we first propose to recognize human attributes using a DVS346 event camera that outputs aligned frame-event streams. This is because event cameras have inherent advantages in high dynamic range, high temporal resolution, and low power consumption. However, event streams contain some noise and are less sensitive to static objects. Therefore, combining them with RGB frame cameras is necessary to achieve more robust and accurate results. Due to the lack of datasets in this area, we first propose a large-scale multi-modal RGB-Event pedestrian attribute recognition benchmark dataset, termed **EventPAR**. This dataset covers common human appearance attributes as well as six human emotional attributes, totaling 50 attributes and 100K paired RGB-Event samples, as shown in Fig. 1. These videos were collected under various challenging scenarios, including different lighting conditions, motion blur, object occlusion, and adverse weather conditions. In addition to natural challenging factors, we also artificially introduced some adversarial attack noises and degradation strategies, such as various types of noise and occlusion. To provide a solid benchmark for future research, we re-train and report 18 mainstream PAR algorithms, as shown in Table 3.

Based on the proposed EventPAR dataset, we introduce a novel multi-modal RGB-Event pedestrian attribute recognition framework leveraging the RWKV model [8], which effectively integrates event streams to further enhance pedestrian attribute recognition results from the traditional RGB frame. Specifically, given the input RGB image and event streams, we first employ an RWKV encoder to extract visual features from both modalities. These features are then fed into an asymmetric RWKV fusion module, designed to better fuse spatial features from RGB frames with temporal information from event streams. This fusion module efficiently removes redundant event tokens while achieving interactive fusion with RGB features. Finally, a linear layer

maps the fused features to multi-label attribute predictions. We extensively validate the proposed framework on three datasets and achieve state-of-the-art performance.

To sum up, we draw the main contributions of this paper as the following three aspects:

1). We propose to recognize the pedestrian attributes using an event camera and construct a large-scale benchmark dataset termed EventPAR. It contains 100K aligned RGB frame and event streams, collected from multiple scenarios, illuminations, etc.

2). We propose a novel RWKV-based framework for the frame-event fusion based attribute recognition. A novel asymmetric RWKV fusion module fuses the RGB frame and event streams effectively and efficiently.

3). We build a large-scale benchmark for the EventPAR dataset by re-training 18 representative and strong PAR algorithms. This benchmark will be a good platform to boost the development of event-based attribute recognition further.

In addition, we also conduct extensive experiments on three PAR benchmark datasets, including the newly proposed EventPAR, MARS-Attribute and DukeMTMC-VID-Attribute dataset. More experiments fully validated the effectiveness of our proposed model for the frame-event pedestrian attribute recognition.

2. Related Works

2.1. Pedestrian Attribute Recognition

Pedestrian Attribute Recognition aims to identify and classify multiple attributes of pedestrians, such as age, gender, clothing type, and accessories, from images or videos. For image-based PAR tasks, CLEAR [1] combines pre-trained language models to generate pseudo-descriptions for attribute queries and extracts robust features using Cross Transformers and adapters. HPNet [29] and DAHAR [49] focus on attribute-related regions via attention mechanisms. PARformer [9] extracts features by combining global and local perspectives. VTB [5] introduces a text encoder for pedestrian attribute recognition tasks. Visual Prompt Tuning (VPT) [16] and CLIP-Adapter [11] enhance few-shot recognition performance by fine-tuning frozen backbones and combining original CLIP knowledge with limited-shot knowledge, respectively.

Video-based PAR, compared to image-based methods, is a relatively new research topic. Researchers have introduced multi-task models, temporal pooling, and sparse temporal attention modules, among other techniques. Chen et al. [3] proposed a multi-task model with an attention module to handle each attribute per frame. Specker et al. [38] introduced global features to incorporate information from different frames. Li et al. [21] proposed a sparse temporal attention module to select unobstructed frames, en-

hancing robustness. Thakare et al. [40] calculated the mutual correlations of attribute predictions from pedestrian images across different views, while Liu et al. [30] introduced a spatio-temporal saliency module to capture correlations between attributes in both spatial and temporal domains. Different from these works, this paper firstly exploits the multi-modal PAR task using the event camera and proposes a large-scale benchmark dataset and RWKV-based framework for this task.

2.2. Event-based Vision

Event cameras have been widely used in computer vision and multi-modal related tasks. Specifically, in the image restoration and enhancement tasks, EventSR [41] proposes a novel end-to-end super-resolution image reconstruction framework that reconstructs low-resolution images from event streams, enhances image quality, and upsamples the enhanced images. EG-VSR [31] learns spatial-temporal coordinates and implicit neural representations from RGB frames and event features, leveraging the high temporal resolution of events to achieve video super-resolution at arbitrary resolutions. Jiang et al. [18] and colleagues have introduced a method that effectively restores motion-blurred video sequences from event-based camera data, achieving this by integrating global and local scale visual and temporal knowledge, along with a differentiable directional event filtering module. Jiang et al. [17] proposed a posterior attention module that adjusts standard attention using the prior knowledge provided by event data, which improves the segmentation performance for moving objects. Inspired by these works, in this paper, we attempt to achieve high-performance PAR by fusing the event stream and RGB frames.

2.3. RWKV Model

The Receptance Weighted Key Value (RWKV) [33] model was first proposed in the field of natural language processing (NLP). Before the emergence of RWKV, Transformers were extensively used in NLP. However, Transformers suffer from quadratic time complexity with respect to sequence length, which significantly limits their efficiency, particularly when processing long sequences. Inspired by the linear attention mechanism in the Attention Free Transformer (AFT) [37], RWKV introduced the WKV attention mechanism. At the same time, the token shift operation was proposed to capture local context. This combination allows RWKV to take advantage of both the parallel processing attention mechanism of Transformers and the sequential time-series pattern of Recurrent Neural Networks (RNNs). Vision-RWKV [58] then extended the RWKV model to the computer vision field. BSBP-RWKV [51] proposes an efficient medical image segmentation framework that integrates Perona-Malik Diffusion for noise sup-

pression with boundary preservation and an RWKV-based architecture to reduce computational complexity. RWKV-SAM [56] proposes an efficient segment-anything framework with a mixed convolution-RWKV backbone and multiscale token decoder, using a joint training benchmark to achieve twice the inference speed and superior segmentation quality compared to Transformer and vision Mamba baselines. Different from these works, this paper first adopts the RWKV model for the pedestrian attribute recognition task.

3. EventPAR Benchmark Dataset

3.1. Protocols

In this work, we follow the guidelines below when constructing the EventPAR benchmark dataset: **1). Multi-Modal:** Unlike existing frame-based PAR datasets, we utilize the DVS346 camera for data collection, obtaining spatiotemporal aligned multi-modal data comprising visible light and event streams. It is the first multi-modal PAR database, laying a solid data foundation for subsequent research. **2). Emotion Attributes:** Unlike conventional PAR datasets that primarily focus on pedestrians' appearance attributes, our new dataset incorporates six fundamental human emotional attributes, i.e., *Happiness*, *Sadness*, *Anger*, *Surprise*, *Fear*, and *Disgust*. This addition effectively fills the gap in the attribute recognition domain by addressing the lack of discussion on the emotional analysis dimension. **3). Diverse Scenes and Cross-Seasonal:** Different from existing PAR datasets that involve short-term data collection, our data acquisition spanned several months, encompassing data from different seasons (summer and winter). Additionally, it covers a variety of scenes and weather conditions, such as daytime and nighttime scenes, as well as weather conditions like sunny and rainy days. These elements significantly enhance the diversity and challenge of the dataset, providing better validation of a model's fitting ability and generalization capability. **4). Large Scale:** It contains 100K pedestrian samples, 12 attribute groups, and 50 fine-grained pedestrian attributes. It is one of the largest PAR datasets, comparable to PA100K in scale. **5). Simulated Complex Real-world Environments:** Our dataset is carefully designed to incorporate a wide range of challenges, such as variations in illumination, motion blur, object occlusion, and adverse weather conditions, all of which simulate the complex real-world difficulties encountered in pedestrian attribute recognition. To further increase the complexity and practical relevance of the dataset, we employ *adversarial attack* techniques [2, 32, 59] during data processing, adding an extra layer of difficulty. This approach not only enhances the robustness of pedestrian attribute recognition technologies but also ensures their applicability in real-world scenarios, as shown in Fig. 2.

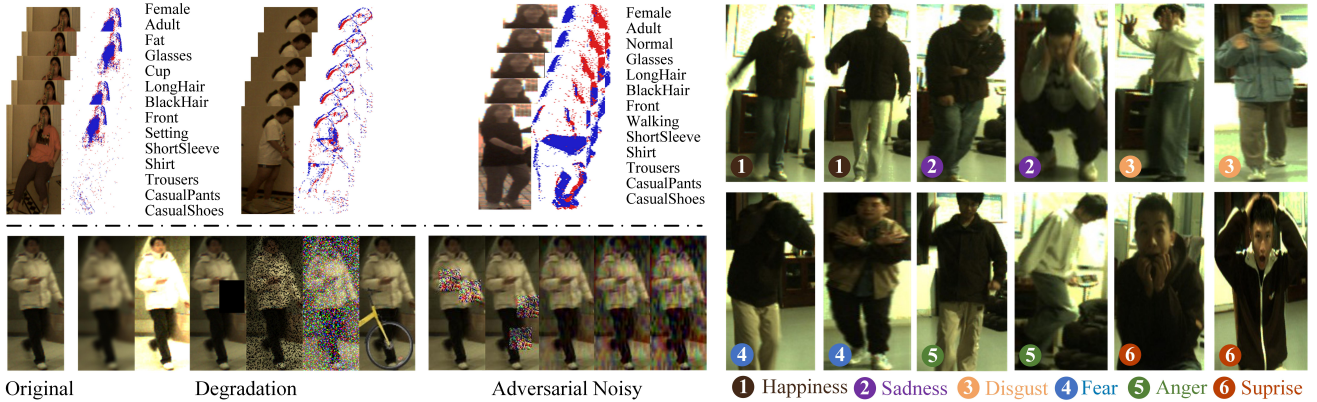


Figure 2. An illustration of representative samples in our newly proposed EventPAR dataset. The left side displays RGB and Event bimodal data collected during summer and winter seasons, as well as the synthetic challenges incorporated into the dataset. The right side presents examples of the six emotion-related attributes.

Table 1. Comparison with existing PAR benchmark datasets. #Att. is short for the number of Attributes. Deg and Adv is short for Degradation and Adversary, respectively.

Dataset	Year	#Att.	#Samples	Video	Frame	Event	Emotion	Deg	Adv
PETA [7]	2014	61	19,000	X	✓	X	X	X	X
WIDER [26]	2016	14	57,524	X	✓	X	X	X	X
RAPv1 [23]	2016	69	41,585	X	✓	X	X	X	X
PA100K [29]	2017	26	100,000	X	✓	X	X	X	X
RAPv2 [24]	2019	76	84,928	X	✓	X	X	X	X
MSP60K [20]	2024	57	60,015	X	✓	X	X	✓	X
MARS-Attribute [61]	2016	43	16,360	✓	X	X	X	X	X
DukeMTMC-VID [34]	2017	36	4,832	✓	X	X	X	X	X
EventPAR (Ours)	2025	50	100,000	✓	✓	✓	✓	✓	✓

Table 2. Attribute groups and details defined in our proposed EventPAR dataset.

Attribute Group	Details
#01 Gender	Male, Female
#02 Age	Child, Adult, Elderly
#03 Body Size	Fat, Normal, Thin
#04 Viewpoint	Front, Back, Side
#05 Head	Long Hair, Black Hair, Hat, Glasses, Mask, Scarf, Headphones
#06 Upper Body	Short Sleeves, Long Sleeves, Shirt, Coat, Cotton-padded Coat
#07 Lower Body	Trousers, Shorts, Jeans, Long Skirt, Short Skirt, Casual Pants, Dress
#08 Shoes	Casual Shoes, Other Shoes
#09 Accessory	Backpack, Shoulder Bag, Hand Bag, Umbrella, Cup, Cellphone
#10 Posture	Walking, Running, Standing, Sitting
#11 Activity	Smoking, Reading
#12 Emotion	Happiness, Sadness, Anger, Surprise, Fear, Disgust

3.2. Data Collection and Annotation

Based on the aforementioned protocols, we collect the EventPAR dataset using a DVS346 event camera, which outputs both RGB frames and event streams. The entire data collection process spanned several months, covering multiple seasons from summer to winter. Approximately 20 students participated in the data collection and subsequent annotation process. As shown in Table 1, our dataset contains 100K spatio-temporal aligned RGB frames and event streams. Each sample in our dataset is annotated with 50 at-

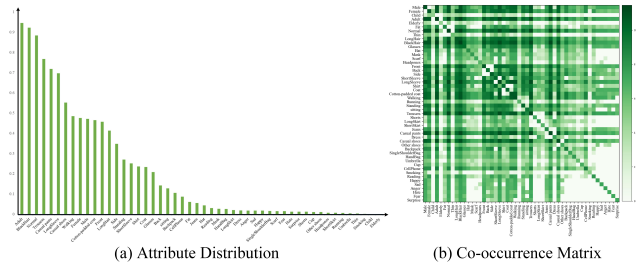


Figure 3. (a) Attributes Distribution: Bar graph showing the prevalence of individual attributes across the dataset; (b) Co-occurrence Matrix of Attributes: Logarithmic heatmap showing the co-occurrence frequency of attribute pairs.

tributes and can be divided into 12 attribute groups, including Gender, Age, Body Size, Viewpoint, Head, Upper Body, Lower Body, Shoes, Accessory, Posture, Activity, and Emotion. More details can be found in Table 2.

By following the MSP60K dataset [20], we also introduced the data quality degradation strategy to evaluate the robustness of models against challenging factors, including changes in lighting, random occlusions, blurring, noise, and adversarial disturbance. Our dataset also exhibits a long-tail distribution, as depicted in Fig. 3 (a), which aligns with the attribute distribution typically observed in real-world data. It is evident that attributes such as *Adult*, *Back Hair*, and *Normal Size* are among the top-3 most frequent, while attributes like *Smoking*, *Child*, and *Elderly* rank at the bottom. We also provide the co-occurrence matrix of our EventPAR dataset as shown in Fig. 3 (b).

3.3. Benchmark Baselines

Based on our newly proposed dataset, we retrained and tested 18 mainstream PAR models, providing a solid baseline for future work on the EventPAR dataset. Specifically,

the following algorithms were included: 1). *CNN-based*: DeepMAR [22], Zhou et al. [62], RethinkPAR [15], SSC-Net [14], SSPNet [36]. 2). *Transformer-based*: DFDT [60], PARFormer [9]. 3). *Mamba-based*: MambaPAR [47], MaHDFT [46]. 4). *Human-Centric Pre-Training Models for PAR*: PLIP [65], HAP [57]. 5). *Visual-Language Models for PAR*: VTB [4], Label2Label [25], PromptPAR [45], SequencePAR [19].

4. Methodology

4.1. Overview

To enhance recognition accuracy and robustness, in this paper, we propose a video-based multi-modal pedestrian attribute recognition framework, as illustrated in Fig. 4. Our method leverages event data as the auxiliary modality to compensate for information loss in the RGB modality under challenging environments, thereby improving the stability of recognition. With the powerful modeling capabilities of Vision-RWKV, we propose an OTN-RWKV guided multi-modal fusion framework. Concretely, we first employ the Visible-RWKV encoder and Event-RWKV encoder to extract the specific features from RGB and event data, respectively. The extracted features are subsequently processed by the proposed OTN-RWKV fusion module to facilitate the interaction and integration of multimodal information. The resulting fused representation is then passed to a classifier for accurate attribute prediction. Please refer to the following for more detailed information.

4.2. Network Architecture

• **Input Encoding** : In this work, event modality is used to assist the RGB video in overcoming information loss in complex environments. Given a sequence of an RGB video denote as $X_r \in \mathbb{R}^{T \times H \times W \times C}$, where T is the total number of frames, and H, W, C correspond to the height, width, and the number of channels of each frame, respectively. We take event streams as $\mathcal{E} = \{e_1, e_2, \dots, e_M\}$, each event point e_j can be denoted as $\{x, y, t, p\}$, representing spatial coordinates, timestamps, and polarity, respectively. To align with the RGB sequence, we stack the event streams into event frames that are temporally synchronized with the RGB frames based on exposure times. Therefore, we can obtain the event frame sequence $X_e \in \mathbb{R}^{T \times H \times W \times C}$.

By inputting a sequence of RGB frames $X_r \in \mathbb{R}^{T \times H \times W \times C}$ and a corresponding sequence of event frames $X_e \in \mathbb{R}^{T \times H \times W \times C}$, we first apply a partitioning operation to process data for both modalities, transforming each frame into HW/p^2 patches, where p denotes the patch size. Then, the patches are added with Position Embedding (P.E.), which are used to encode spatial information to obtain RGB tokens $X_r \in \mathbb{R}^{T \times N \times C}$ and event tokens $X_e \in \mathbb{R}^{T \times N \times C}$ separately, where N is the number of to-

kens.

• **RWKV Encoder**: In this paper, we employ Vision-RWKV [8] as our visual encoder, which adopts a block-stacked design with L layers to enhance its encoding capability, where each block consists of a Spatial-Mix module and a Channel-Mix module. In each layer, RGB tokens $X_r \in \mathbb{R}^{T \times N \times C}$ and event visual tokens $X_e \in \mathbb{R}^{T \times N \times C}$ are first fed into the Spatial-Mix module, which performs linear complexity global attention computation. Specifically, as shown in the top right of Fig. 4, the input visual tokens first undergo a token Shift operation to capture local context information before being fed into three parallel linear layers to obtain the matrices $R_s, K_s, V_s \in \mathbb{R}^{T \times N \times C}$. The formulas are as follows,

$$\begin{aligned} R_s &= \text{Q-Shift}_R(X_i)W_R, \\ K_s &= \text{Q-Shift}_K(X_i)W_K, \\ V_s &= \text{Q-Shift}_V(X_i)W_V, \quad i \in (r, e) \end{aligned} \quad (1)$$

where the Q-Shift function is a specialized token shift mechanism specifically designed for vision tasks. After that, K_s and V_s are used to calculate the global attention result $wkv \in \mathbb{R}^{T \times N \times C}$ by the Bi-WKV module, which is a linear complexity bidirectional attention mechanism. Subsequently, the wkv is multiplied with $\sigma(R)$, which controls the output O_i probability,

$$\begin{aligned} O_i &= (\sigma(R_s) \odot wkv)W_O, \\ wkv &= \text{Bi-WKV}(K_s, V_s), \quad i \in (r, e), \end{aligned} \quad (2)$$

where the operator σ represents the sigmoid function, while \odot denotes element-wise multiplication. After the output linear projection, the features are subjected to layer normalization to enhance stability and facilitate effective training.

Subsequently, the tokens are fed into the Channel-Mix module to achieve channel-wise fusion, as shown in the bottom right of Fig. 4. The parameters R_c and K_c are computed similarly to the Spatial-Mix before the final output,

$$\begin{aligned} R_c &= \text{Q-Shift}_R(O_i)W_R, \\ K_c &= \text{Q-Shift}_K(O_i)W_K, \end{aligned} \quad (3)$$

the gating mechanism $\sigma(R_c)$ is used to modulate the output O'_i . To maintain information integrity and promote gradient flow, residual connections are introduced to fuse the module outputs, thereby effectively alleviating the vanishing gradient problem. This process can be expressed as,

$$\begin{aligned} O'_i &= (\sigma(R_c) \odot V_c)W_O, \\ V_c &= \text{SquaredReLU}(K_c)W_V, \end{aligned} \quad (4)$$

• **OTN-RWKV**: Due to the asynchronous nature of event cameras, the event streams tend to be highly dense, resulting in stacked event frames containing a significant amount of

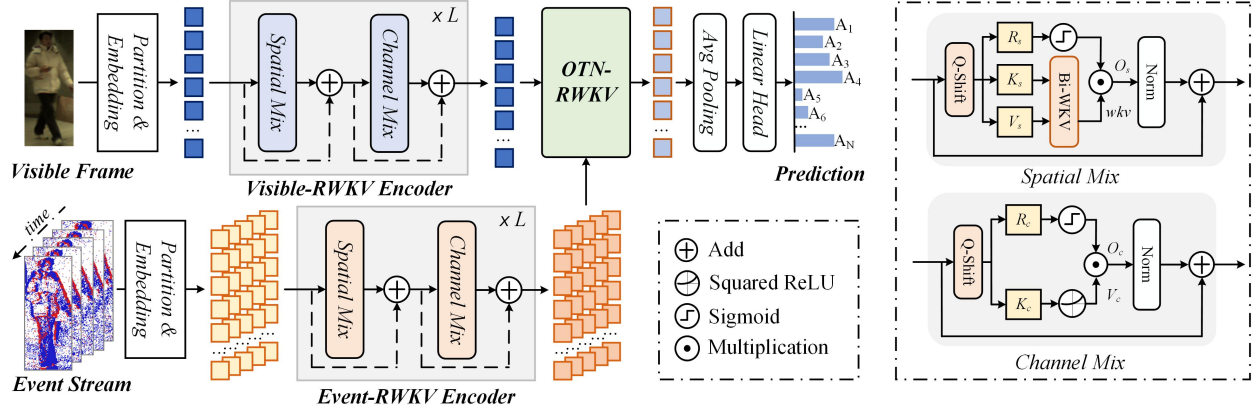


Figure 4. An overview of our proposed OTN-RWKV guided RGB-Event fusion for pedestrian attribute recognition.

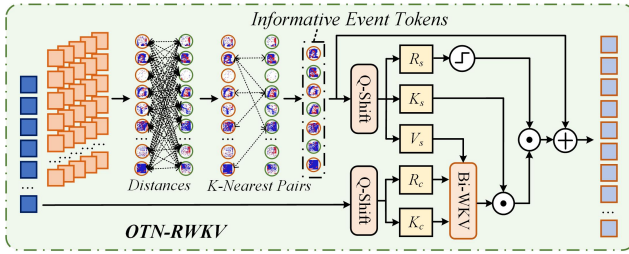


Figure 5. Illustration of our proposed OTN-RWKV for RGB-Event fusion.

redundant information. This redundancy not only increases computational overhead but also causes information ambiguity, thereby diminishing the effectiveness of event data as auxiliary information. To address this issue, we propose the OTN-RWKV fusion module, which first applies the similarity-based filtering on the visual tokens output O'_e of event modality, removing highly redundant tokens and achieving one-to-N multimodal fusion. Specifically, a similarity matrix is employed to identify the top- K most similar token pairs, from which only the most representative tokens are retained. This approach enhances data efficiency and improves the quality of multimodal fusion. The implementation process is as follows,

$$O''_e = \text{KNP}_{filter}(\text{sim}(O'_e, O'_e)) \odot O'_e, \quad (5)$$

where $O''_e \in \mathbb{R}^{N' \times C}$ represents the tokens for the informative filtered event. After filtering, both modalities are aligned to have the same number of tokens, facilitating effective multimodal fusion.

Although traditional fusion methods (e.g., concatenation, addition, and 1×1 convolution) generally exhibit strong compatibility and generalization across different models, they frequently result in information loss, limiting their effectiveness in preserving fine-grained multi-

modal details. Inspired by the concept of cross attention and LCR[54], in this work, we further propose a novel interactive fusion strategy. As shown in Fig. 5, we first apply the Q-shift operation separately to the two types of visual tokens, corresponding to Eq. 1 and Eq. 3, respectively. Subsequently, V_s , R_c , and K_c are used to compute the cross-attention results through a linear complexity bidirectional attention mechanism,

$$O_{fusion} = \sigma(R_s) \odot LN(K_s \odot \text{Bi-WKV}) + O'_e, \quad (6)$$

$$\text{Bi-WKV}(R, K, V)_t = \frac{\sum_{i=0, i \neq t}^M e^{-(|t-i|-1)/M \cdot v_s + r_i} k_i + e^{u+r_t} k_t}{\sum_{i=0, i \neq t}^M e^{-(|t-i|-1)/M \cdot v_s + r_i} + e^{u+r_t}}. \quad (7)$$

where t represents the t -th token of the input, M represents the total number of tokens, u is a C-dimensional learnable vector that acts as a bonus indicating the current token, and LN refers to LayerNorm. Unlike LCR[54], which uses the learnable vector w , we replace w with the output V_s from Eq. 1 to better focus on the current sample.

4.3. Loss Function

After the effective fusion of the two modalities using the OTN-RWKV module, the resulting representation is fed into an average pooling layer and then a linear classification head, yielding the final attribute prediction P_{attr} . In the training phase, we adopt the weighted cross-entropy loss (WCE Loss)[4] to alleviate the distribution imbalance between pedestrian attributes, which is widely used by attribute recognition,

$$\mathcal{L}_{wce} = -\frac{1}{N} \sum_{i=1}^N \sum_{j=1}^M \omega_j (y_{ij} \log(p_{ij}) + (1 - y_{ij}) \log(1 - p_{ij})), \quad (8)$$

here, N represents the total number of samples, M denotes the number of attributes, and ω_j is the weight for the j -th attribute. y_{ij} and p_{ij} denote the ground truth and predicted result, respectively.

5. Experiments

5.1. Datasets & Evaluation Metric

In this study, we conduct a comprehensive benchmark of 18 pedestrian attribute recognition methods, representing the most important models in the field of pedestrian attribute recognition. Additionally, the performance of our method is compared with existing state-of-the-art (SOTA) pedestrian attribute recognition (PAR) methods across our benchmark and two publicly available datasets: MARS-Attribute Dataset [61] and DukeMTMC-VID-Attribute Dataset [34].

- **MARS-Attribute Dataset** is an annotated dataset for pedestrian attribute recognition, containing multiple multi-label and binary attributes such as pedestrian action, orientation, clothing color, gender, and others. These attributes are decomposed into 43 binary attributes to enhance the performance of pedestrian attribute recognition models for training and testing. The dataset is divided into a training subset and a testing subset, with 8,298 and 8,062 tracklets, respectively. Each tracklet contains approximately 60 frames on average. The dataset includes 625 and 626 distinct pedestrian identities for training and testing.

- **DukeMTMC-VID-Attribute Dataset** is an extension of the DukeMTMC-VID dataset, specifically designed for pedestrian attribute recognition. This dataset includes various annotated pedestrian attributes aimed at improving pedestrian re-identification performance. It features 2,032 identities and 16,522 video sequences captured across multiple scenarios, with a focus on real-world and challenging environments. In addition, the dataset provides rich attribute annotations. By splitting the multi-label attributes into binary attributes, the dataset includes a total of 36 binary attributes for training and testing. The training subset contains 702 distinct pedestrian identities and 16,522 images, while the testing subset includes 17,661 images corresponding to 702 pedestrians. The DukeMTMC-VID-Attribute dataset is widely used for evaluating attribute-based pedestrian re-identification models, offering valuable insights into how attributes influence recognition accuracy under varying conditions.

For the evaluation of our and the compared PAR models, we use five widely adopted evaluation metrics to assess performance, including: **mean Accuracy** (mA), **Accuracy** (Acc), **Precision** (Prec), **Recall**, and **F1-score** (F1), which can be expressed as:

$$Accuracy = \frac{TP + TN}{FP + FN + TP + TN} \quad (9)$$

$$Precision = \frac{TP}{FP + TP}, \quad Recall = \frac{TP}{TP + FN} \quad (10)$$

$$F1 = \frac{2 \times Recall \times Precision}{Recall + Precision} \quad (11)$$

where TP denotes the number of correctly predicted positive samples, TN is the number of correctly predicted neg-

ative samples, FP and FN denote the number of false positive and false negative samples, respectively.

5.2. Implementation Details

In our experiments, we use the VRWKV6-B version of the VRWKL [8] base model pre-trained on the ImageNet-1K [6] dataset as the visual encoder. This version consists of 12 block layers. We select SGD [12] as the optimizer, We leverage the warm-up strategy and increase the learning rate from 0 to the initial learning rate 0.008 linearly in the first 10 epochs, and decrease the learning rate by a factor of 0.1 when the number of iterations increases, we set the batch size to 16 and train for 60 epochs, the filtering threshold is set to 0.75. During both the training and inference stages, we first pad and resize the images to 256×128. Training images are augmented with random horizontal flipping with a probability of 0.5 and random cropping with a padding size of 10. Feature interaction is performed using the last layer of the transformer. Our model is implemented based on the PyTorch deep learning framework, and the experiments are conducted on a server equipped with an NVIDIA RTX 3090 GPU. For more details about our framework, please refer to our source code.

5.3. Comparison on Public Datasets

In this section, we conduct a detailed comparison between our model and existing pedestrian attribute recognition (PAR) algorithms on three benchmark datasets. Since the MARS-Attribute and DukeMTMC-VID-Attribute datasets contain only the RGB modality, we simulate the corresponding event data to ensure the completeness and fairness of the experiments.

- **Results on EventPAR Dataset.** We collect and analyze public PAR methods from 2015 to 2024 on the EventPAR dataset as shown in Table 3, methods such as HAP [57], SequencePAR [19], and PARFormer [9] have demonstrated superior performance. Among them, the HAP method achieved outstanding results, with mA, Acc, Prec, Recall, and F1 scores of 77.33, 74.13, 83.99, 80.56, and 82.24, respectively. Our method achieves strong performance with mA, Acc, Prec, Recall, and F1 scores of 79.32, 76.00, 82.37, 84.55, and 83.22, respectively, outperforming existing approaches across most evaluation metrics. Furthermore, by incorporating the event auxiliary modality, our model further improves these scores to 87.66, 84.78, 89.03, 89.38, and 89.07, achieving the best overall results. These experimental findings on the EventPAR dataset not only confirm the effectiveness of our method in pedestrian attribute recognition tasks but also highlight the significant advantage of integrating event modality in enhancing model robustness under complex real-world conditions.

- **Results on MARS-Attribute Dataset [61].** As shown in Table 4, to further evaluate the generalization and effec-

Table 3. Comparison with public methods on our datasets. The **first** and **second** are shown in **red** and **blue**, Size indicates the size of checkpoint file, and **#MS** means the GPU memory used for optimization, Test time refers to the time spent on the test set.

Methods	Publish	Code	mA	Acc	Prec	Recall	F1	Test Time	Params (MB)	Flops (GB)	Size (MB)	#MS (MB)
#01 DeepMAR [22]	ACPR15	URL	71.15	72.39	86.42	78.93	82.51	46s	23	4	181	846
#02 ALM [39]	ICCV19	URL	71.31	68.80	78.82	75.97	77.37	21s	17	45	66	484
#03 Strong Baseline [15]	arXiv20	URL	73.75	70.63	81.34	78.26	79.32	91s	24	4	91	788
#04 RethinkingPAR [15]	arXiv20	URL	71.23	69.00	80.80	77.16	78.94	57s	24	4	91	105
#05 SSCNet [14]	ICCV21	URL	72.12	69.95	78.36	80.10	79.22	24s	24	3	90	854
#06 VTB [4]	TCSVT22	URL	76.96	73.81	80.74	83.15	81.67	441s	93	15	333	114
#07 Label2Label [25]	ECCV22	URL	72.47	69.54	78.75	79.14	78.55	43s	66	12	829	3788
#08 DFDT [60]	EAAI22	URL	70.14	70.95	78.71	81.82	80.24	193s	88	26	669	1884
#09 Zhou et al. [62]	IJCAI23	URL	70.16	67.41	79.76	76.40	78.04	76s	140	15	536	4176
#10 PARFormer [9]	TCSVT23	URL	75.33	74.21	79.33	85.82	82.09	732s	195	68	756	11634
#11 SequencePAR [19]	arXiv23	URL	73.96	73.40	81.47	81.17	81.11	275s	466	413	1776	11263
#12 VTB-PLIP [65]	arXiv23	URL	73.72	71.50	79.97	80.57	79.99	26s	31	8	591	1614
#13 Rethink-PLIP [65]	arXiv23	URL	57.91	62.78	78.27	70.81	74.35	44s	24	4	144	80
#14 PromptPAR [45]	TCSVT24	URL	74.92	71.79	78.33	83.01	80.31	977s	8	3	1200	4435
#15 SSPNet [63]	PR24	URL	71.71	69.41	80.46	77.46	78.93	32s	26	7	100	1240
#16 HAP [57]	NIPS24	URL	77.33	74.13	83.99	80.56	82.24	92s	86	17	327	2683
#17 MambaPAR [47]	arXiv24	URL	72.28	70.57	77.99	81.70	79.50	18s	26	1	98	116
#18 MaHDFT [46]	arXiv24	URL	75.54	72.27	80.28	82.19	80.59	158s	158	3978	431	187
Ours	-	-	79.32	76.00	82.37	84.55	83.22	68s	107	39	429	2200
Ours+E	-	-	87.66	84.78	89.03	89.38	89.07	361s	201	77	836	2312

tiveness of our method, we conducted comprehensive experiments on another public dataset, comparing it with several state-of-the-art approaches. While our method did not consistently achieve the top performance across all metrics, it demonstrated strong competitiveness, achieving 73.74, 80.43, 84.63, and 82.18 in Accuracy, Precision, Recall, and F1, respectively. These results reflect a balanced performance with high accuracy and effective attribute capture.

• **Results on DukeMTMC-VID-Attribute Dataset [34].** Our method achieves performance comparable to mainstream approaches on this dataset, with mA, Accuracy, Precision, Recall, and F1 of 68.19, 82.83, 77.30, 79.38, and 78.32, respectively. Although the overall performance is slightly lower than that of the VTB method, our approach still demonstrates solid generalization ability and stability. Notably, it achieves competitive results while maintaining relatively low computational complexity, validating the effectiveness and feasibility of our proposed method. These findings suggest that our method remains competitive in certain real-world scenarios and has the potential for further improvement through optimization of the model architecture and fusion strategy.

5.4. Ablation Study

In this section, we conduct a comprehensive ablation study on the core modules of EventPAR, including different input configurations, various backbone architectures, fusion strategies, event data aggregation methods, and the threshold settings in the similarity-based filtering mechanism.

• **Analysis of different input settings.** In this study, we varied the number of RGB inputs and conducted extensive experiments, as shown in Table 5. The first two rows repre-

sent RGB-only and Event-only inputs, both yielding strong results. RGB performed slightly worse due to added perturbations. When combining RGB and Event, performance improved, demonstrating their complementarity. However, excessive RGB inputs led to performance drops, likely due to redundant features and preprocessing noise. These factors increased the burden during feature extraction, introduced irrelevant cues, and weakened the ability to capture essential semantic information, ultimately degrading recognition performance.

• **Analysis of different aggregation strategies of Event.** As shown in the first part of Table 8, we systematically compared four event data aggregation strategies: Max Pooling, Mean Pooling, a graph-based GNN, and our proposed Similarity-based approach. While Max and Mean pooling offer efficient but coarse feature representations, GNN captures structural dependencies with stronger expressive power. Our Similarity-based method adaptively fuses features based on semantic similarity between event frames, effectively retaining discriminative temporal information and filtering noise. In terms of mA 87.59, Accuracy 84.80, and F1 89.10, it outperformed all other strategies, hereby validating the effectiveness of our proposed similarity-based aggregation strategy.

• **Analysis of different threshold setting in the similarity aggregation strategies** To further validate the impact of threshold settings in the similarity-based filtering strategy, we conducted experiments with varying similarity thresholds under identical conditions. The threshold controls the degree of fusion between event frames, preserving only those with sufficient semantic similarity to reduce redundant or noisy features. As shown in Table 7, a well-chosen

Table 4. Results on MARS-Attribute and DukeMTMC-VID-Attribute RGB-Event based PAR dataset.

Methods	Backbone	MARS-Attribute Dataset				DukeMTMC-VID-Attribute Dataset			
		Accuracy	Precision	Recall	F1	Accuracy	Precision	Recall	F1
VTB [4]	ViT-B/16	72.73	82.79	83.52	82.89	72.50	83.60	82.24	82.38
Zhou et al. [62]	ConvNext	69.43	81.75	80.64	81.19	65.51	78.42	77.40	77.91
VTB-PLIP [65]	ResNet50	54.93	70.02	69.23	69.14	43.95	60.80	58.52	59.10
Rethink-PLIP [65]	ResNet50	47.85	62.15	64.80	63.45	40.25	55.41	56.13	55.77
SSPNet [63]	ResNet50	65.68	77.09	79.74	78.39	67.53	78.54	79.78	79.15
MambaPAR [47]	Vim	69.07	81.83	79.39	80.24	61.55	75.54	74.84	74.24
Ours	RWKV-B	73.74	80.43	84.63	82.18	68.19	82.83	77.30	79.38

Table 5. Comparison of different input settings and filtering threshold is set to 0.95.

RGB	Event	mA	Acc	Prec	Recall	F1
1	0	79.32	76.00	82.37	84.55	83.22
0	5	87.10	84.49	89.03	89.07	88.91
1	5	87.66	84.78	89.03	89.38	89.07
3	5	85.95	81.87	86.80	86.95	86.56
5	5	85.67	82.20	87.13	86.86	86.72

Table 6. Comparison of different feature fusion methods.

Method	mA	Acc	Prec	Recall	F1
Concat	87.63	84.60	88.80	89.40	88.96
Add	87.17	84.62	88.96	89.30	88.99
1 × 1 Conv	83.77	80.33	84.78	88.63	86.44
OTN-RWKV	87.66	84.78	89.03	89.38	89.07

Table 7. Comparison of different threshold setting in the feature filtering module.

Threshold	mA	Acc	Prec	Recall	F1
0.60	87.23	84.04	88.62	88.91	88.62
0.65	87.55	84.16	88.62	89.09	88.70
0.70	87.68	83.93	88.32	89.11	88.71
0.75	87.66	84.78	89.03	89.38	89.07
0.80	87.70	84.13	88.75	88.92	88.69
0.85	87.72	84.74	88.99	89.40	89.05
0.95	86.55	82.43	87.32	87.44	87.05

threshold better preserves discriminative features and enhances performance, while extreme thresholds may impair fusion quality and degrade results.

• **Analysis of different feature fusion methods.** We adopted two fusion strategies: holistic fusion and stepwise fusion. The corresponding results are shown in Table 6 and the second part of Table 8, respectively. We compared our proposed OTN-RWKV fusion strategy with three common methods: Concat, Add, and 1×1Conv. Although Concat increases feature dimensionality, it fails to capture inter-

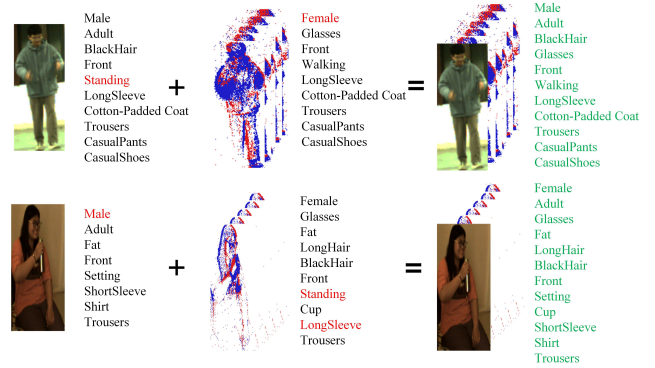


Figure 6. Visualization of pedestrian attributes predicted by our proposed method. The red attributes indicate incorrect predictions, while green attributes represent ground truth.

modal relationships. Add struggles with modality discrepancies, and 1×1Conv may lead to the loss of semantic details. In contrast, OTN-RWKV achieved superior performance in both fusion modes. It recorded mA of 87.66, ACC of 84.78, and F1 of 89.07 in holistic fusion, and mA of 87.38, ACC of 84.82, and F1 of 89.10 in stepwise fusion, outperforming all baseline methods. By finely integrating RGB and event modality features, the proposed strategy effectively captures their complementarity, significantly improves model robustness and overall performance, and fully validates its effectiveness.

• **Analysis of different backbone.** To further evaluate the effectiveness of the proposed RWKV model, we conducted comparative experiments with ViT and ResNet-50 under identical settings. ViT captures global context, while ResNet-50 focuses on local features. In contrast, RWKV combines the strengths of RNNs and Transformers, achieving a balance between long-range dependency modeling and efficiency. Using consistent inputs and training protocols, our RWKV model outperformed both backbones with mA, Accuracy, and F1 of 87.66, 84.78, and 89.10, respectively, as shown in the third part of Table 8, highlighting its superiority in pedestrian attribute recognition.

Table 8. Ablation study of different backbones and framework modules on the EventPAR dataset.

No.	Backbone	Aggregation				Fusion				EventPAR Dataset		
		Max	Mean	Gnn	Similarity	Concat	Add	1x1Conv	OTN-RWKV	mA	Acc	F1
01	RWKV	✓				✓				87.56	84.62	88.98
02	RWKV		✓			✓				87.50	84.68	89.01
03	RWKV			✓		✓				84.53	82.24	87.50
04	RWKV				✓	✓				87.59	84.80	89.10
05	RWKV		✓			✓				87.50	84.68	89.01
06	RWKV		✓				✓			86.92	84.45	88.88
07	RWKV		✓					✓		87.13	84.40	88.86
08	RWKV		✓						✓	87.38	84.82	89.10
09	ViT				✓				✓	84.05	82.41	87.60
10	ResNet50				✓				✓	83.85	82.45	87.64
11	RWKV				✓				✓	87.66	84.78	89.07

5.5. Visualization

• **Visualization of Predicted Results.** As shown in Fig. 6, we present a visualization of attribute prediction results using different input modalities: RGB only, Event only, and the fused bimodal input. In the figure, green text represents the ground truth attributes, while red text indicates incorrectly predicted ones. The results show that using a single modality, whether the RGB data with added noise or the Event data alone, cannot achieve comprehensive and accurate predictions. In contrast, when both modalities are combined, the model can better capture complementary information, which significantly improves the accuracy and robustness of attribute recognition.

• **Visualization of Aggregation Strategy.** To provide an intuitive understanding of our proposed similarity-based aggregation strategy, we present a visual illustration in Fig. 7. In this figure, the colored regions represent event tokens that are retained and contribute to the final aggregation, while the black areas indicate tokens filtered out by the similarity-based selection process. As shown, the strategy effectively suppresses redundant or irrelevant information by adaptively retaining only semantically relevant tokens. This helps the model focus on discriminative patterns, thereby improving the overall recognition performance.

6. Conclusion and Future Works

In this paper, we addressed the limitations of existing pedestrian attribute recognition (PAR) methods, which are predominantly based on RGB frame cameras and suffer from challenges such as sensitivity to lighting conditions and motion blur. Moreover, current approaches focus primarily on external appearance and clothing attributes, neglecting the emotional dimensions of pedestrians. To overcome these constraints, we introduced a novel multi-modal RGB-Event attribute recognition task, leveraging the advantages

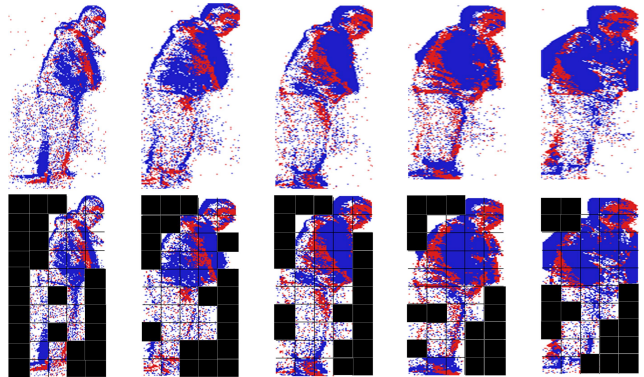


Figure 7. Illustration of our proposed similarity-based aggregation strategy for event token selection, where the black parts indicate the filtered-out tokens.

of event cameras in low-light, high-speed, and low-power scenarios. Our key contribution is the creation of EventPAR, the first large-scale multi-modal PAR dataset, which includes 100K paired RGB-Event samples covering 50 attributes related to both appearance and six human emotions. By retraining and evaluating mainstream PAR models on EventPAR, we established a comprehensive benchmark, offering valuable data and algorithmic baselines for the community. Furthermore, we proposed a novel RWKV-based multi-modal PAR framework, incorporating an RWKV visual encoder and an asymmetric RWKV fusion module. Extensive experiments conducted on EventPAR and two simulated datasets demonstrated state-of-the-art performance, underscoring the effectiveness of our approach.

In our future works, we will focus on exploiting learning-based new event representations for the perception of event streams for pedestrian attribute recognition.

References

- [1] Doanh C Bui, Thinh V Le, Ba Hung Ngo, and Tae Jong Choi. Clear: Cross-transformers with pre-trained language model is all you need for person attribute recognition and retrieval. *arXiv preprint arXiv:2403.06119*, 2024.
- [2] Nicholas Carlini and David Wagner. Towards evaluating the robustness of neural networks. In *2017 IEEE Symposium on Security and Privacy (SP)*, pages 39–57. Ieee, 2017.
- [3] Zhiyuan Chen, Annan Li, and Yunhong Wang. A temporal attentive approach for video-based pedestrian attribute recognition. In *Pattern Recognition and Computer Vision: Second Chinese Conference, PRCV 2019, Xi'an, China, November 8–11, 2019, Proceedings, Part II 2*, pages 209–220. Springer, 2019.
- [4] Xinhua Cheng, Mengxi Jia, Qian Wang, and Jian Zhang. A simple visual-textual baseline for pedestrian attribute recognition. *IEEE Transactions on Circuits and Systems for Video Technology*, 2022.
- [5] Xinhua Cheng, Mengxi Jia, Qian Wang, and Jian Zhang. A simple visual-textual baseline for pedestrian attribute recognition. *IEEE Transactions on Circuits and Systems for Video Technology*, 32(10):6994–7004, 2022.
- [6] Jia Deng, Wei Dong, Richard Socher, Li-Jia Li, Kai Li, and Li Fei-Fei. Imagenet: A large-scale hierarchical image database. In *2009 IEEE conference on computer vision and pattern recognition*, pages 248–255. Ieee, 2009.
- [7] Yubin Deng, Ping Luo, Chen Change Loy, and Xiaoou Tang. Pedestrian attribute recognition at far distance. In *Proceedings of the 22nd ACM international conference on Multimedia*, pages 789–792, 2014.
- [8] Yuchen Duan, Weiyun Wang, Zhe Chen, Xizhou Zhu, Lewei Lu, Tong Lu, Yu Qiao, Hongsheng Li, Jifeng Dai, and Wenhai Wang. Vision-rwkv: Efficient and scalable visual perception with rwkv-like architectures. *arXiv preprint arXiv:2403.02308*, 2024.
- [9] Xinwen Fan, Yukang Zhang, Yang Lu, and Hanzhi Wang. Parformer: Transformer-based multi-task network for pedestrian attribute recognition. *IEEE Transactions on Circuits and Systems for Video Technology*, 34(1):411–423, 2023.
- [10] Hiren Galiyawala and Mehul S Raval. Person retrieval in surveillance using textual query: a review. *Multimedia Tools and Applications*, 80(18):27343–27383, 2021.
- [11] Peng Gao, Shijie Geng, Renrui Zhang, Teli Ma, Rongyao Fang, Yongfeng Zhang, Hongsheng Li, and Yu Qiao. Clip-adapter: Better vision-language models with feature adapters. *International Journal of Computer Vision*, 132(2): 581–595, 2024.
- [12] Robert Mansel Gower, Nicolas Loizou, Xun Qian, Alibek Sailanbayev, Egor Shulgin, and Peter Richtárik. Sgd: General analysis and improved rates. In *International conference on machine learning*, pages 5200–5209. PMLR, 2019.
- [13] Peixian Hong, Tao Wu, Ancong Wu, Xintong Han, and Wei-Shi Zheng. Fine-grained shape-appearance mutual learning for cloth-changing person re-identification. In *Proceedings of the IEEE/CVF conference on computer vision and pattern recognition*, pages 10513–10522, 2021.
- [14] Jian Jia, Xiaotang Chen, and Kaiqi Huang. Spatial and semantic consistency regularizations for pedestrian attribute recognition. In *Proceedings of the IEEE/CVF international conference on computer vision*, pages 962–971, 2021.
- [15] Jian Jia, Houjing Huang, Xiaotang Chen, and Kaiqi Huang. Rethinking of pedestrian attribute recognition: A reliable evaluation under zero-shot pedestrian identity setting. *arXiv preprint arXiv:2107.03576*, 2021.
- [16] Menglin Jia, Luming Tang, Bor-Chun Chen, Claire Cardie, Serge Belongie, Bharath Hariharan, and Ser-Nam Lim. Visual prompt tuning. In *European Conference on Computer Vision*, pages 709–727. Springer, 2022.
- [17] Zexi Jia, Kaichao You, Weihua He, Yang Tian, Yongxiang Feng, Yaoyuan Wang, Xu Jia, Yihang Lou, Jingyi Zhang, Guoqi Li, et al. Event-based semantic segmentation with posterior attention. *IEEE Transactions on Image Processing*, 32:1829–1842, 2023.
- [18] Zhe Jiang, Yu Zhang, Dongqing Zou, Jimmy Ren, Jiancheng Lv, and Yebin Liu. Learning event-based motion deblurring. In *Proceedings of the IEEE/CVF Conference on Computer Vision and Pattern Recognition*, pages 3320–3329, 2020.
- [19] Jiandong Jin, Xiao Wang, Chenglong Li, Lili Huang, and Jin Tang. Sequencepar: Understanding pedestrian attributes via a sequence generation paradigm. *arXiv preprint arXiv:2312.01640*, 2023.
- [20] Jiandong Jin, Xiao Wang, Qian Zhu, Haiyang Wang, and Chenglong Li. Pedestrian attribute recognition: A new benchmark dataset and a large language model augmented framework. *arXiv preprint arXiv:2408.09720*, 2024.
- [21] Geonu Lee, Kimin Yun, and Jungchan Cho. Robust pedestrian attribute recognition using group sparsity for occlusion videos. *arXiv preprint arXiv:2110.08708*, 2021.
- [22] Dangwei Li, Xiaotang Chen, and Kaiqi Huang. Multi-attribute learning for pedestrian attribute recognition in surveillance scenarios. In *2015 3rd IAPR Asian Conference on Pattern Recognition (ACPR)*, pages 111–115, 2015.
- [23] Dangwei Li, Zhang Zhang, Xiaotang Chen, Haibin Ling, and Kaiqi Huang. A richly annotated dataset for pedestrian attribute recognition. *arXiv preprint arXiv:1603.07054*, 2016.
- [24] Dangwei Li, Zhang Zhang, Xiaotang Chen, and Kaiqi Huang. A richly annotated pedestrian dataset for person retrieval in real surveillance scenarios. *IEEE transactions on image processing*, 28(4):1575–1590, 2018.
- [25] Wanhua Li, Zhexuan Cao, Jianjiang Feng, Jie Zhou, and Jiwen Lu. Label2label: A language modeling framework for multi-attribute learning. In *European Conference on Computer Vision*, pages 562–579. Springer, 2022.
- [26] Yining Li, Chen Huang, Chen Change Loy, and Xiaoou Tang. Human attribute recognition by deep hierarchical contexts. In *Computer Vision—ECCV 2016: 14th European Conference, Amsterdam, The Netherlands, October 11–14, 2016, Proceedings, Part VI 14*, pages 684–700. Springer, 2016.
- [27] Yu-Lei Li. Unsupervised embedding and association network for multi-object tracking. In *IJCAI*, pages 1123–1129, 2022.
- [28] Kai Liu, Sheng Jin, Zhihang Fu, Ze Chen, Rongxin Jiang, and Jieping Ye. Uncertainty-aware unsupervised multi-

- object tracking. In *Proceedings of the IEEE/CVF International Conference on Computer Vision*, pages 9996–10005, 2023.
- [29] Xihui Liu, Haiyu Zhao, Maoqing Tian, Lu Sheng, Jing Shao, Shuai Yi, Junjie Yan, and Xiaogang Wang. Hydraplus-net: Attentive deep features for pedestrian analysis. In *Proceedings of the IEEE international conference on computer vision*, pages 350–359, 2017.
- [30] Zhenyu Liu, Da Li, Xinyu Zhang, Zhang Zhang, Peng Zhang, Caifeng Shan, and Jungong Han. Pedestrian attribute recognition via spatio-temporal relationship learning for visual surveillance. *ACM Transactions on Multimedia Computing, Communications and Applications*, 20(6):1–15, 2024.
- [31] Yunfan Lu, Zipeng Wang, Minjie Liu, Hongjian Wang, and Lin Wang. Learning spatial-temporal implicit neural representations for event-guided video super-resolution. In *Proceedings of the IEEE/CVF Conference on Computer Vision and Pattern Recognition*, pages 1557–1567, 2023.
- [32] Seyed-Mohsen Moosavi-Dezfooli, Alhussein Fawzi, and Pascal Frossard. Deepfool: a simple and accurate method to fool deep neural networks. In *Proceedings of the IEEE conference on computer vision and pattern recognition*, pages 2574–2582, 2016.
- [33] Bo Peng, Eric Alcaide, Quentin Anthony, Alon Albalak, Samuel Arcadinho, Stella Biderman, Huanqi Cao, Xin Cheng, Michael Chung, Matteo Grella, et al. Rwkv: Reinventing rnns for the transformer era. *arXiv preprint arXiv:2305.13048*, 2023.
- [34] Ergys Ristani, Francesco Solera, Roger Zou, Rita Cucchiara, and Carlo Tomasi. Performance measures and a data set for multi-target, multi-camera tracking. In *European conference on computer vision*, pages 17–35. Springer, 2016.
- [35] Ziyu Shan, Yujie Zhang, Qi Yang, Haichen Yang, Yiling Xu, Jenq-Neng Hwang, Xiaozhong Xu, and Shan Liu. Contrastive pre-training with multi-view fusion for no-reference point cloud quality assessment. In *Proceedings of the IEEE/CVF Conference on Computer Vision and Pattern Recognition*, pages 25942–25951, 2024.
- [36] Jifeng Shen, Teng Guo, Xin Zuo, Heng Fan, and Wankou Yang. Sspnet: Scale and spatial priors guided generalizable and interpretable pedestrian attribute recognition. *Pattern Recognition*, 148:110194, 2024.
- [37] Nitish Srivastava Chen Huang Hanlin Goh Ruixiang Zhang Shuangfei Zhai, Walter Talbott and Josh Susskind. An attention free transformer. *arXiv preprint arXiv:2105.14103*, 2021.
- [38] Andreas Specker, Arne Schumann, and Jürgen Beyerer. An evaluation of design choices for pedestrian attribute recognition in video. In *2020 IEEE International Conference on Image Processing (ICIP)*, pages 2331–2335. IEEE, 2020.
- [39] Chufeng Tang, Lu Sheng, Zhaoxiang Zhang, and Xiaolin Hu. Improving pedestrian attribute recognition with weakly-supervised multi-scale attribute-specific localization. In *Proceedings of the IEEE/CVF International Conference on Computer Vision*, pages 4997–5006, 2019.
- [40] Kamalakar Vijay Thakare, Debi Prasad Dogra, Heeseung Choi, Haksun Kim, and Ig-Jae Kim. Let’s observe them over time: An improved pedestrian attribute recognition approach. In *Proceedings of the IEEE/CVF Winter Conference on Applications of Computer Vision*, pages 708–717, 2024.
- [41] Lin Wang, Tae-Kyun Kim, and Kuk-Jin Yoon. Eventsr: From asynchronous events to image reconstruction, restoration, and super-resolution via end-to-end adversarial learning. In *Proceedings of the IEEE/CVF conference on computer vision and pattern recognition*, pages 8315–8325, 2020.
- [42] Pengfei Wang, Changxing Ding, Wentao Tan, Mingming Gong, Kui Jia, and Dacheng Tao. Uncertainty-aware clustering for unsupervised domain adaptive object re-identification. *IEEE Transactions on Multimedia*, 25:2624–2635, 2022.
- [43] Tai Wang, ZHU Xinge, Jiangmiao Pang, and Dahua Lin. Probabilistic and geometric depth: Detecting objects in perspective. In *Conference on Robot Learning*, pages 1475–1485. PMLR, 2022.
- [44] Xiao Wang, Shaofei Zheng, Rui Yang, Aihua Zheng, Zhe Chen, Jin Tang, and Bin Luo. Pedestrian attribute recognition: A survey. *Pattern Recognition*, 121:108220, 2022.
- [45] Xiao Wang, Jiandong Jin, Chenglong Li, Jin Tang, Cheng Zhang, and Wei Wang. Pedestrian attribute recognition via clip based prompt vision-language fusion. *arXiv preprint arXiv:2312.10692*, 2023.
- [46] Xiao Wang, Weizhe Kong, Jiandong Jin, Shiao Wang, Rui-chong Gao, Qingchuan Ma, Chenglong Li, and Jin Tang. An empirical study of mamba-based pedestrian attribute recognition, 2024.
- [47] Xiao Wang, Shiao Wang, Yuhe Ding, Yuehang Li, Wentao Wu, Yao Rong, Weizhe Kong, Ju Huang, Shihao Li, Haoxiang Yang, et al. State space model for new-generation network alternative to transformers: A survey. *arXiv preprint arXiv:2404.09516*, 2024.
- [48] Zhenyu Wang, Ya-Li Li, Xi Chen, Hengshuang Zhao, and Shengjin Wang. Uni3detr: Unified 3d detection transformer. *Advances in Neural Information Processing Systems*, 36: 39876–39896, 2023.
- [49] Mingda Wu, Di Huang, Yuanfang Guo, and Yunhong Wang. Distraction-aware feature learning for human attribute recognition via coarse-to-fine attention mechanism. In *Proceedings of the AAAI conference on artificial intelligence*, pages 12394–12401, 2020.
- [50] Haoran Xu, Peixi Peng, Guang Tan, Yuan Li, Xinhai Xu, and Yonghong Tian. Dmr: Decomposed multi-modality representations for frames and events fusion in visual reinforcement learning. In *Proceedings of the IEEE/CVF Conference on Computer Vision and Pattern Recognition*, pages 26508–26518, 2024.
- [51] Tianxiang Chen Xudong Zhou. Bsbp-rwkv: Background suppression with boundary preservation for efficient medical image segmentation. *ACM Multimedia*, 2024.
- [52] Yujie Xue, Ruihui Li, Fan Wu, Zhuo Tang, Kenli Li, and Mingxing Duan. Bi-ssc: Geometric-semantic bidirectional fusion for camera-based 3d semantic scene completion. In *Proceedings of the IEEE/CVF Conference on Computer Vision and Pattern Recognition*, pages 20124–20134, 2024.
- [53] Shuyu Yang, Yinan Zhou, Zhedong Zheng, Yaxiong Wang, Li Zhu, and Yujiao Wu. Towards unified text-based person

- retrieval: A large-scale multi-attribute and language search benchmark. In *Proceedings of the 31st ACM International Conference on Multimedia*, pages 4492–4501, 2023.
- [54] Zhuowen Yin, Chengru Li, and Xingbo Dong. Video rwkv: Video action recognition based rwkv. *arXiv preprint arXiv:2411.05636*, 2024.
- [55] Shijie Yu, Shihua Li, Dapeng Chen, Rui Zhao, Junjie Yan, and Yu Qiao. Cocas: A large-scale clothes changing person dataset for re-identification. In *Proceedings of the IEEE/CVF conference on computer vision and pattern recognition*, pages 3400–3409, 2020.
- [56] Haobo Yuan, Xiangtai Li, Lu Qi, Tao Zhang, Ming-Hsuan Yang, Shuicheng Yan, and Chen Change Loy. Mamba or rwkv: Exploring high-quality and high-efficiency segment anything model. *arXiv preprint arXiv:2406.19369*, 2024.
- [57] Junkun Yuan, Xinyu Zhang, Hao Zhou, Jian Wang, Zhongwei Qiu, Zhiyin Shao, Shaofeng Zhang, Sifan Long, Kun Kuang, Kun Yao, et al. Hap: Structure-aware masked image modeling for human-centric perception. *Advances in Neural Information Processing Systems*, 36, 2024.
- [58] Zhe Chen Xizhou Zhu Lewei Lu Tong Lu Yu Qiao Hongsheng Li Jifeng Dai Yuchen Duan, Weiyun Wang and Wenhai Wang. Vision-rwkv: Efficient and scalable visual perception with rwkv-like architectures. *arXiv preprint arXiv:2403.02308*, 2024.
- [59] Yutong Zhang, Yao Li, Yin Li, and Zhichang Guo. A review of adversarial attacks in computer vision. *arXiv preprint arXiv:2308.07673*, 2023.
- [60] Aihua Zheng, Huimin Wang, Jiayang Wang, Huaibo Huang, Ran He, and Amir Hussain. Diverse features discovery transformer for pedestrian attribute recognition. *Engineering Applications of Artificial Intelligence*, 119:105708, 2023.
- [61] Liang Zheng, Zhi Bie, Yifan Sun, Jingdong Wang, Chi Su, Shengjin Wang, and Qi Tian. Mars: A video benchmark for large-scale person re-identification. In *Computer Vision—ECCV 2016: 14th European Conference, Amsterdam, The Netherlands, October 11–14, 2016, Proceedings, Part VI 14*, pages 868–884. Springer, 2016.
- [62] Yibo Zhou, Hai-Miao Hu, Jinzuo Yu, Zhenbo Xu, Weiqing Lu, and Yuran Cao. A solution to co-occurrence bias: Attributes disentanglement via mutual information minimization for pedestrian attribute recognition. *arXiv preprint arXiv:2307.15252*, 2023.
- [63] Yibo Zhou, Hai-Miao Hu, Yirong Xiang, Xiaokang Zhang, and Haotian Wu. Pedestrian attribute recognition as label-balanced multi-label learning. *arXiv preprint arXiv:2405.04858*, 2024.
- [64] Aichun Zhu, Zijie Wang, Yifeng Li, Xili Wan, Jing Jin, Tian Wang, Fangqiang Hu, and Gang Hua. Dssl: Deep surroundings-person separation learning for text-based person retrieval. In *Proceedings of the 29th ACM international conference on multimedia*, pages 209–217, 2021.
- [65] Jialong Zuo, Changqian Yu, Nong Sang, and Changxin Gao. Plip: Language-image pre-training for person representation learning. *arXiv preprint arXiv:2305.08386*, 2023.